

Theoretical Analysis of CO₂ Adducts on the Native E'' Center in Ion-Bombarded Porous Silica

Nazzareno Re and Antonio Sgamellotti*

Dipartimento di Chimica, Università di Perugia, Via Elce di Sotto 8, 06123 Perugia, Italy

Gianfranco Cerofolini

SGS-Thomson Microelectronics, 20041 Agrate, Italy

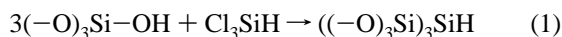
Received: April 28, 1997; In Final Form: August 12, 1997[®]

Density functional calculations have been performed on molecular models of silica defects and their CO₂ adducts. The results are consistent with a previous experimental infrared characterization, which was interpreted in terms of CO₂ addition to the SiO₂ skeleton at the diradical silicon defect produced by argon bombardment. According to this interpretation, the addition of CO₂ takes place first via the formation of a carboxylate group which, after annealing, evolves to an ester species and then to a carboxylic acid after exposure to wet air. The geometries and thermodynamical stabilities of the proposed species and other possible adducts have been evaluated. The calculated carbonyl stretching frequencies are in good agreement with the experimental values and confirm the validity of the previous interpretation, adding further details and clarifying a few doubtful assignments.

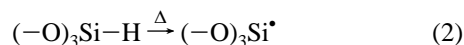
1. Introduction

Due to unsaturated forces which are manifested at their surfaces, highly dispersed solids usually have a high reactivity. Porous silica, however, is usually characterized by a high chemical inertness even at very high dispersion. The combination of inertness and low preparation cost render porous silica an ideal candidate as a support in heterogeneous catalysis.

For most applications porous silica is obtained via a sol–gel technique, which allows control of porosity, surface area, silanol terminations, etc.¹ Additional properties can be imparted to silica by suitable processing. Reactive silica is usually obtained only through high-temperature processing. We briefly mention three processes for the preparation of reactive silica. (1) Morterra et al.^{2,3} started from alkoxylated silica, i.e. silica with isolated –OR (R = alkyl) termination, whose heat treatment in a vacuum produced a highly reactive material, whose reactivity is essentially of a radical nature. (2) Another method, proposed for homogeneously doped materials, consists in the insertion during gelling of Si–H groups in the SiO₂ skeleton via the reaction



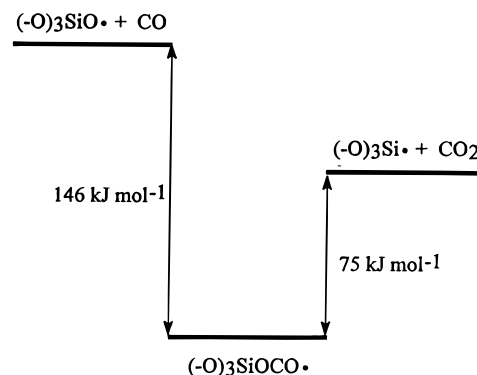
followed by a pyrolysis of the Si–H bond:^{5,6}



(3) Another way to prepare reactive silica is simply to heat at very high temperature, in such a way as to eliminate most silanol terminations. Siloxanic bridges are indeed formed, but they may be very strained and are easily cleaved by atmosphere molecules.

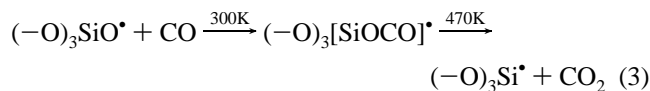
Radtig and co-workers⁷ developed in the late 1970s a technique for the preparation of reactive silica surfaces via crushing in an inert atmosphere. Through combined adsorption, calorimetric, and electronic paramagnetic resonance (EPR) studies, they showed that this reactive SiO₂ surface is essentially characterized by three active sites: (1) the strained disiloxane

SCHEME 1



center $(-O)_3Si\cdots O\cdots Si(O^-)_3$, (2) the $(-O)_3Si\cdot$ radical, and (3) the $(-O)_3SiO\cdot$ radical.

In addition, starting from the observation that the $(-O)_3Si\cdot$ practically does not react with CO at 300 K, they developed a process for the almost complete transformation of the $(-O)_3SiO\cdot$ center into the $(-O)_3Si\cdot$ center,

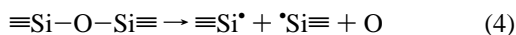


determined the energies of the above states (see Scheme 1), and attributed to the radical $(-O)_3[SiOCO]\cdot$ the oxygen-attached structure $(-O)_3Si-OC\cdot O$ rather than the carbon-attached structure $(-O)_3Si-C(O)O\cdot$ (this attribution contrasts with that expected from the known reactivity of the CO₂ species).

A method for the preparation of highly specific defective sites in porous silica has recently been proposed by Cerofolini and co-workers.⁸ In this approach the dispersed silica is bombarded with an energetic ion-beam. Due to the short-range nature of the interaction involved in the stopping of energetic ions, momentum transfer is possible only for collision with a low impact parameter so that simultaneous displacement of two or more adjacent atoms is very rare and can be neglected. The

[®] Abstract published in *Advance ACS Abstracts*, October 1, 1997.

bombardment is therefore expected to produce only the oxygen bridge vacancy

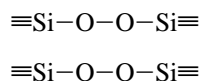


(usually referred to as the E'' center) and the silicon link vacancy (SLV sketched in Scheme 2) in addition to atomic oxygen and silicon. In the bombardment of condensed materials most of the displaced atoms remain in the proximity of the site where they were generated, thereby allowing a fast recovery of the radiation damage. The basic idea was that *if the bombarded target is at the same time dispersed and reticulate, the imparted damage is not recovered and the silica network is not destroyed*. Of course, since the E'' and SLV defects were expected to be strongly reactive, the bombardment was carried out in a controlled atmosphere, to extract information on the hosting site from the formed adducts.

2. Experimental Evidence

The addition of CO_2 into ion-bombarded porous SiO_2 was studied by implanting $^{40}\text{Ar}^{2+}$ at an acceleration voltage of 150 kV and at a fluence of $5 \times 10^{14} \text{ cm}^{-2}$ onto a porous silica target kept under a CO_2 atmosphere.⁸ The bombarded sample was subsequently annealed at 500 °C for 1 h in a vacuum and then exposed to wet air. Fourier transform infrared (IR) absorption measurements were carried out on (i) as-prepared bombarded samples; (ii) annealed samples and (iii) wet-air exposed samples. As-prepared samples gave evidence for a sharp band, located at 1515 cm^{-1} , and another, broad band, extending from 1595 to 1715 cm^{-1} consisting of two unresolved peaks in the spectral regions $1595\text{--}1630 \text{ cm}^{-1}$ and $1680\text{--}1715 \text{ cm}^{-1}$; see Figure 1a. Annealing at 500 °C led to a decrease of the band at 1515 cm^{-1} and a simultaneous increase of a band around 1700 cm^{-1} . In ref 8 only the difference between the spectrum of the annealed sample and that of the as-implanted silica was reported, which led to the net band at 1734 cm^{-1} ; see Figure 1b. Actually, a better look at the original spectra of the annealed sample shows a broad band from 1595 to 1750 cm^{-1} (see Figure 1a), with a shape similar to the $1595\text{--}1715 \text{ cm}^{-1}$ band observed for the as-implanted sample. More in detail, the two peaks that form this broad band are now better resolved than before annealing, and there is a variation of their relative intensities, with an increase of the second peak at $1680\text{--}1750 \text{ cm}^{-1}$. Moreover the latter peak shows a small shift and a more pronounced tail toward higher frequencies. Exposure to wet air led to the disappearance of this broad band at $1595\text{--}1750 \text{ cm}^{-1}$ and the progressive rise of a more intense band at 1705 cm^{-1} ; see Figure 1c. Another heat treatment at 500 °C in vacuum destroyed the latter signal at 1705 cm^{-1} , and only a broad band in the region $1700\text{--}1740 \text{ cm}^{-1}$ reappeared. Reexposure of the sample to wet air resulted in the progressive rise of the band at 1705 cm^{-1} ; see Figure 1d.

This bombardment experiment in a CO_2 atmosphere permits the study of the CO_2 addition to the E'' center. This idea stood on the assumption that the tetraradical SLV relaxes to a peroxidated silicon vacancy (PSV) defect



whose interaction with CO_2 can be ignored. The validity of this assumption is in principle doubtful, because in the presence of SLV CO_2 might give extravagant peroxo-carbosilicates, like those reported in Figure 2. The infrared spectroscopic analysis of the bombarded sample, however, did not give any indication

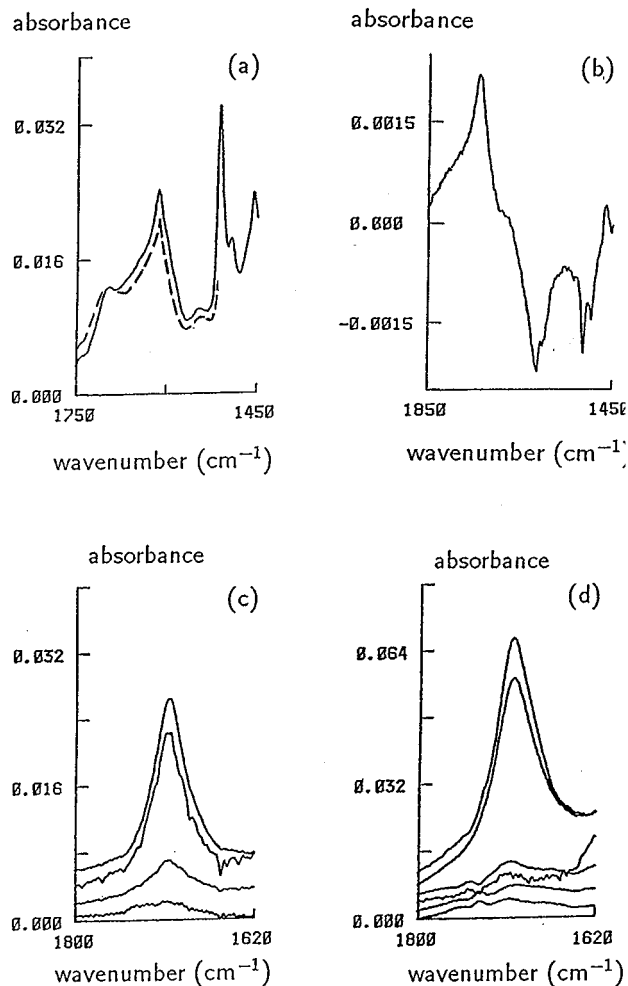


Figure 1. (a) Difference IR spectra obtained for as-bombarded sample (—), and annealed sample (---); (b) spectrum obtained by subtracting the spectrum of bombarded silica from that of annealed silica; (c) difference spectra obtained after different exposure times to wet air of the annealed sample; and (d) difference spectra obtained after annealing at 500 °C and reexposure to wet air of the sample in part c.

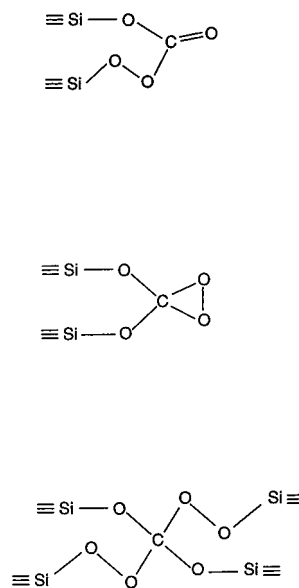
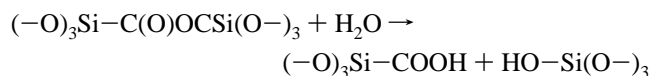


Figure 2. Possible peroxo-carbonate species.

supporting their presence (possibly because the probe is not suited for that). Rather, the observed IR data were interpreted by assuming that

(i) the addition of CO_2 occurs via the formation of a

carboxylate group, $(-\text{O})_3\text{Si}-\text{COO}^- + \text{Si}(\text{O}-)_3$; (ii) the carboxylate forms an ester-like group, $(-\text{O})_3\text{Si}-\text{C}(\text{O})\text{O}-\text{Si}(\text{O}-)_3$, after heating at 500 °C; and (iii) the ester group undergoes hydrolysis after exposure to wet air, forming a carboxylic acid:



More in detail, the peak at 1515 cm⁻¹ observed in the as-implanted sample was ascribed to the antisymmetric C=O stretching of the carboxylate ion $-\text{COO}^-$, while the broad band in the region 1595–1715 cm⁻¹ was assigned to hydrogen-bonded carbonyl stretching. The band at 1734 cm⁻¹ observed in the difference spectrum of the annealed sample was attributed to the C=O stretching of the ester group $\equiv\text{Si}-\text{CO}-\text{O}-\text{Si}\equiv$, and the intense band at 1705 cm⁻¹ observed in the wet air exposed sample was ascribed to the C=O stretching of a carboxylic group $-\text{COOH}$. However, these attributions were somewhat doubtful because organosilicon carboxylic derivatives (like $\equiv\text{Si}-\text{COOH}$, $\equiv\text{Si}-\text{C}(\text{O})\text{O}-$, $\equiv\text{Si}-\text{COO}-$) are not known and are considered to be unstable.

3. Models and Theoretical Methods

To support the above attributions, Car–Parrinello molecular dynamics simulations of the collision at high energy were performed and confirmed the original interpretation.⁹ However, molecular dynamics techniques are not suitable for accurate calculations of spectroscopic data (like vibrational frequencies) or thermodynamic data (like relative stabilities of the various configurations and acidity of the Si–COOH site), which could instead be deduced from experiments. In this work we have therefore performed *ab initio* density functional (DFT) calculations on suitable models of the silica defects and their CO₂ adducts to give a quantitative account of the experimental data of ref 8. Following the experimental indications which do not support the presence of peroxo-carbosilicates, we did not consider the interaction of CO₂ with SLV defects, thus assuming their complete relaxation to stable PSV centers (see the discussion in the previous paragraph). We therefore limited our attention to the interaction of CO₂ with the *E'* center. To model the silicon *E'* defect, we have used two $(\text{OH})_3\text{Si}\cdot$ molecular radicals, while the proposed CO₂ adducts were modeled by the corresponding molecular compounds in which the silica centers have been substituted by $(\text{OH})_3\text{Si}-$ groups (see below). Such an approach in which small discrete molecules are employed to simulate the behavior of solid substructures has been applied to several systems.¹⁰ The main drawback of this approach is that it neglects any interaction within the three-dimensional framework of the solid, and this is not always a realistic approximation. However, it has been successfully employed to simulate the behavior of silica, silicate functional groups, zeolites, and surface silica hydroxyls.^{11–14} Some of the CO₂ adducts on the *E'* defects proposed in this work involve an ester bridge between two silicon atoms and have been modeled by molecules with two silicon atoms such as $(\text{HO})_3\text{Si}-\text{CO}-\text{O}-\text{Si}(\text{OH})_3$. Unfortunately, such a molecular model allows a complete relaxation of the two $\text{Si}(\text{OH})_3$ groups, at variance with the actual situation in the solid silica, where a full relaxation is hampered by the rigid structure of the three-dimensional network. We have therefore employed more realistic structural models of the actual silica structure, based on a cyclic molecule with two or three silicon atoms connected by siloxanic bridges; see below.

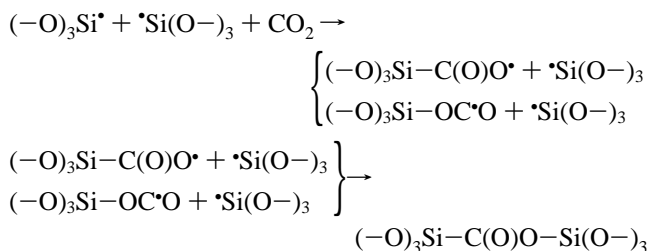
The calculations reported in this paper have been performed by the Gaussian 94 program package¹⁵ and were done on IBM

RISC/6000 workstations. A gradient-corrected functional for exchange–correlation potential and energy was used, based on the Vosko–Wilk–Nusair parametrization for homogeneous electron gas correlation¹⁶ and including Becke's nonlocal correction to the local exchange expression¹⁷ and the nonlocal correction for the correlation energy provided by the functional of Lee, Young, and Parr.¹⁸ We used two basis sets of valence double- ζ and triple- ζ level augmented by polarization functions. A standard 6-31G* basis set was used for all geometry optimizations and harmonic frequencies calculations. Single-point calculations with a 6-311G** basis set have been performed on the stationary points and employed in the computation of the thermodynamic stabilities. Full geometry optimizations were performed on the considered model molecules using the nonlocal functional described above. It has already been demonstrated that this density functional gives accurate optimized geometries of first- and second-row compounds, and for large basis sets as those employed, accurate bond energies.^{19,20}

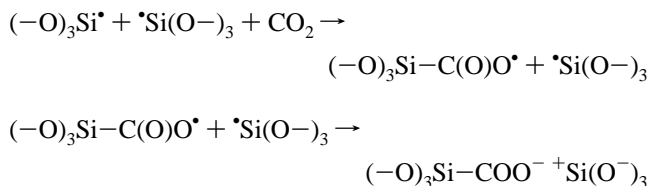
Harmonic normal-mode frequencies have been calculated for the optimized structures, computing analytical energy second derivatives as programmed in Gaussian 94. It has recently been shown for a reference group of 122 molecules that DFT methods including nonlocal potentials give harmonic frequencies in good agreement with experiment, with overall root-mean-square (rms) errors in the range 34–48 cm⁻¹.²¹ Following ref 21, we scaled the calculated frequencies by an optimum scaling factor, 0.9940, obtained by minimizing the residual errors between the experimental and calculated harmonic frequencies (using a BLYP functional and a 6-31G* basis set).

4. Results and Discussion

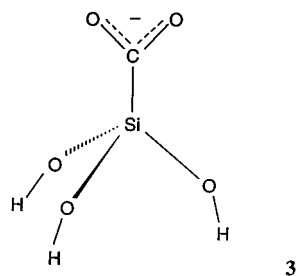
4.1. Expected *E'* Adducts. The *E'* center associated with the oxygen bridge vacancy is expected to be strongly reactive. Two possible pathways can be hypothesized for its reaction with a CO₂ molecule. For a suitable large Si–Si distance within the *E'* center, the reaction pathway is expected to involve the consecutive reactions of each of its constituting radicals leading to the eventual formation of an ester-like group.



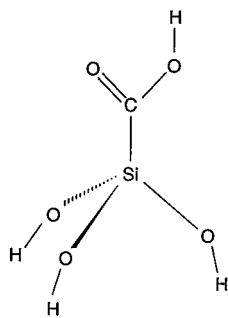
Although two possible radicals can be obtained from the reaction between the CO₂ and one radical, i.e. $(-\text{O})_3\text{Si}-\text{C}(\text{O})\text{O}\cdot$ and $(-\text{O})_3\text{Si}-\text{OC}\cdot\text{O}$, the final product is the same ester-like group. For Si–Si distances not suitable to allow the formation of an ester bridge, the addition of the CO₂ to one silicon radical may be followed by an electron transfer from the other radical and the formation of a ionic pair,



constituted by a carboxylate anion and a silicon cation.



3



7

Figure 3. Geometries of the considered model molecules of carboxylate, **3**, and carboxylic acid, **7**, species.

TABLE 1: Main Optimized Geometrical Parameters for the Model Molecules 3 and 7

	3	7
Si-C	1.93	1.93
C-O	1.28	1.23/1.38
Si-O	1.68	1.65
(Si)O-H	0.98	0.98
(C)O-H		0.99
O-C-O	130	122
Si-C-O	115	109
C-Si-O	115	107
Si-O-H	101	110
C-O-H		106

4.2. Interpretation of the IR Data. Following the lines of ref 8, we excluded the formation of unstable radical species and first considered the formation of an ionic pair with the negative charge on the CO₂-approached site. We considered isolated anionic adducts as the simplest model of this ionic pair. The CO₂ molecule may approach silicon with either a carbon or oxygen atom. The two routes would lead, respectively, to the proposed carboxylate $(-\text{O})_3\text{Si}-\text{COO}^-$ or to $(-\text{O})_3\text{Si}-\text{OCO}^-$ species.

We have first considered the oxygen-attached species, $(-\text{O})_3\text{Si}-\text{Si}-\text{OCO}^-$, performing a geometry optimization on the $(\text{OH})_3\text{Si}-\text{Si}-\text{OCO}^-$ model molecule, **2**. However, no minimum has been found, but only a transition-state structure corresponding to the dissociation into a $(\text{OH})_3\text{Si}-\text{O}^-$ and a CO molecule. This result is in agreement with flowing afterglow and ion cyclotron resonance studies on the gas-phase reaction between H_3Si^- and CO₂ and with Hartree-Fock calculations performed on this system.²² This oxygen-attached adduct can therefore be ruled out.

We have then considered the carboxylate species. A geometrical optimization has been performed on the $(\text{OH})_3\text{Si}-\text{COO}^-$ molecule, **3** (Figure 3), and the results are illustrated in Table 1. The full set of harmonic frequencies have been calculated for the $(\text{OH})_3\text{Si}-\text{COO}^-$ anion, and those concerning the SiCO₂ moiety are reported in Table 2. We see that the

TABLE 2: Harmonic Scaled Frequencies (cm^{-1}) and Intensities (kM cm^{-1}) in Parentheses for the Si-C and Carbonyl Stretching of the Model Molecules 3 and 7

mode assignment	3	7
stretch Si-C	772 (8)	641 (7)
sym stretch CO	1235 (78)	
antisym stretch CO	1512 (333)	
stretch C=O		1263 (3)
stretch C-O		1691 (180)

antisymmetric C=O stretching has been calculated at 1512 cm^{-1} and is very close to the band observed at 1515 cm^{-1} . The symmetric stretching vibration of the carboxylate ion has been calculated at 1235 cm^{-1} , but it cannot be experimentally observed, as this spectral region is completely dominated by the skeletal SiO₂ vibrations.⁸ The same reasons prevented also the observation of the calculated Si-C stretching frequencies reported in Table 2.

As far as the isolated $(\text{OH})_3\text{SiCOO}^-$ anion is considered, no attribution can be assigned to the band in the region $1595-1715 \text{ cm}^{-1}$, experimentally observed for the as-implanted sample. To assign this band, we propose an extension of the original interpretation of ref 8, based on the observation that the average distance between the silicon atoms of a E'' center is around 3.6 \AA and is compatible with the formation of an ester bridge. Therefore, an unrelaxed or weakly relaxed E'' center would give directly a $(-\text{O})_3\text{Si}-\text{C}(\text{O})\text{O}-\text{Si}(\text{O}-)_3$ ester species by interaction with CO₂. We then assigned the band at $1595-1715$ to the C-O stretching of these ester species, attributing the broadening to higher frequencies to strain effects due to the rigid structure of the silica network; see below.

The ester species was first modeled by a $(\text{OH})_3\text{Si}-\text{C}(\text{O})\text{O}-\text{Si}(\text{OH})_3$ molecule, **4** (see Figure 4). A geometry optimization has been performed on **4**, and the corresponding vibrational spectrum calculated (see Tables 3 and 4). Such a model allows a complete relaxation of the two Si(OH)₃ groups and describes a completely unstrained ester bond. The corresponding C=O stretching has been calculated at 1599 cm^{-1} and matches well with the first peak at $1595-1630 \text{ cm}^{-1}$. The broadening of this band to higher frequencies and the appearance of the second weaker peak at $1680-1715 \text{ cm}^{-1}$ can be explained in terms of the strain imposed on the $(-\text{O})_3\text{Si}-\text{C}(\text{O})\text{O}-\text{Si}(\text{O}-)_3$ ester species by the rigid structure of the silica network. It is known that microporous silica is built mainly by three-, four-, five-, and six-membered rings (i.e. cyclic structures made up by three, four, five, or six silicon atoms connected by oxygen atoms; see Figure 5a, illustrating two examples) fused together to form the three-dimensional network.¹ Therefore, when an E'' center is formed by an oxygen displacement, the two silicon radicals were part of an open three-, four-, five-, or six-membered ring; see Figure 5b. The formation of the ester bridge between these two silicon atoms will therefore lead to a silicon-lactone species, as shown in Figure 5c. Now, it is known that the C-O stretching frequencies of organic esters are shifted to higher frequencies in cyclic lactones due to the ring strain, and the effect can be significant for the lower membered rings (up to 80 cm^{-1} for β -lactones), while is almost negligible for higher membered rings (δ -lactones or higher).²³ This led us to attribute the higher frequencies part of the broad band at $1595-1715 \text{ cm}^{-1}$ to lower membered silicon-lactone species. These lactone species, actually fused within the silica three-dimensional network, have been modeled by discrete cyclic molecules. We considered only the most strained species with two and three silicon atoms, **5** and **6** (Figure 4), assuming that the carbonyl stretching in four-membered or higher membered rings is essentially the same as that calculated for the acyclic molecule

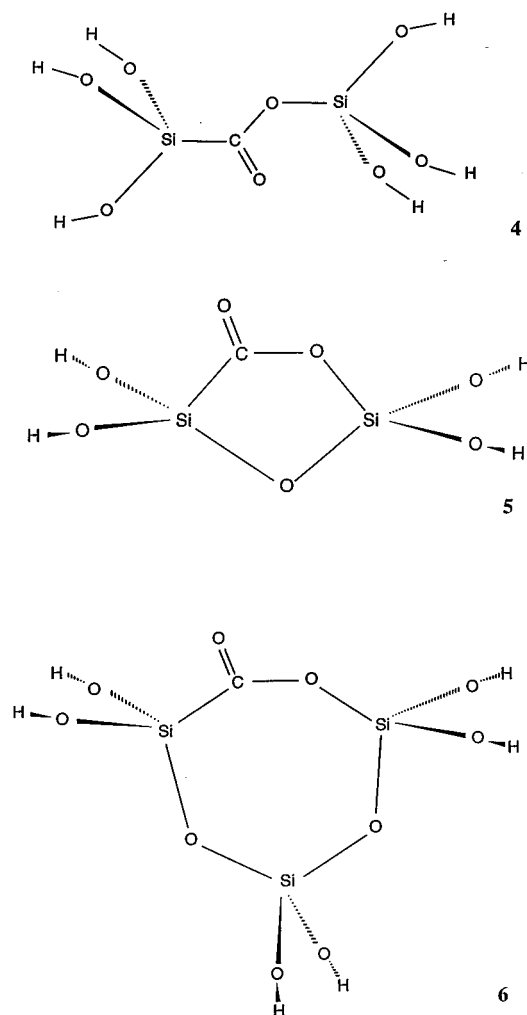


Figure 4. Geometries of the considered model molecules of esterlike species with linear, **4**, and cyclic, **5** and **6**, structures.

TABLE 3: Main Optimized Geometrical Parameters for the Ester Model Molecules 4, 5, and 6

	4	5	6
Si—C	1.93	1.92	1.92
C=O	1.22	1.21	1.22
C—O	1.39	1.43	1.39
Si'—O	1.71	1.69	1.66
Si—C=O	124	131	117
Si—C—O	113	108	123
C—Si—O	108	99	117
O—C—O	121	121	119
C—O—Si'	107	116	145
O—Si'—O(H)	109	105	116

TABLE 4: Harmonic Scaled Frequencies (cm⁻¹) and Intensities (kM cm⁻¹) in Parentheses for the Si—C and Carbonyl Stretching of the Ester Model Molecules 4, 5, and 6

mode assignment	4	5	6
stretch Si—C	591 (3)	541 (34)	608 (25)
stretch C—O	1117 (119)	1152 (196)	1149 (184)
stretch C=O	1599 (152)	1780 (242)	1711 (211)

4. A geometry optimization has been performed on these molecules, and the corresponding vibrational spectra have been calculated; the results are reported in Tables 3 and 4. We see that the C—O stretching frequency calculated for the three-membered molecule **6** is 1711 cm⁻¹, very close to the maximum of the peak at 1680–1715 cm⁻¹. A substantially higher frequency has been calculated for the two-membered cyclic molecule **5** (1780 cm⁻¹, but it is known that two-membered

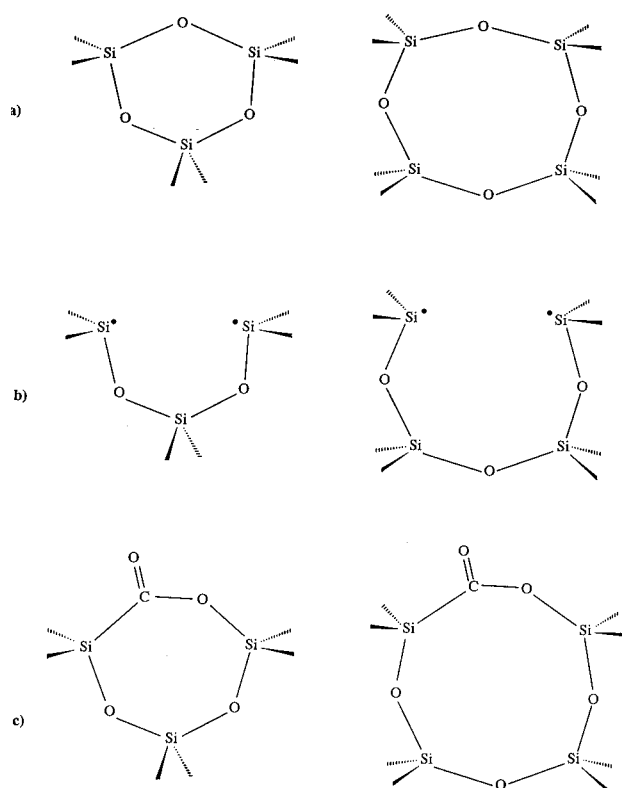


Figure 5. Geometries of (a) the three- and four-membered ring units within the silica framework and their corresponding (b) *E''* defects and (c) cyclic ester species.

rings are very rare in porous silica.¹ Putting together all the results above, we attributed the first peak at 1595–1630 cm⁻¹ of the considered broad band to essentially unstrained ester species (derived by four-membered or higher membered siloxane rings) and the second weaker peak at 1680–1715 cm⁻¹ to a strained silicon-lactone species, presumably a three-membered siloxane ring which is much less abundant. Moreover, a strong broadening of both peaks is expected due to the presence of ring structures of different size and to the several fused-ring systems which can be formed within the silica network and slightly change the strain on the carbonyl group.

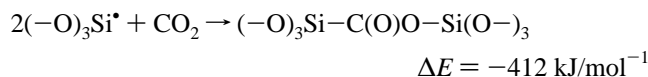
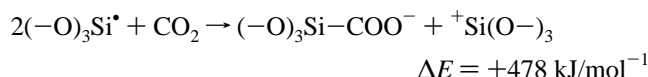
This interpretation of the infrared data for the as-implanted sample can be easily extended to the spectrum of the annealed sample (Figure 1b). In the as-implanted sample only a part of the silicon carboxylate groups first produced by the addition of CO₂ on one of the two silicon radicals of the *E''* defects form an ester bridge with the vicinal silicon radical. A significant number of carboxylate groups is observed, presumably because a partial relaxation of the *E''* defects has displaced the two silicon radicals too close to form an ester bond. Due to the annealing, there is a structural rearrangement of the silica three-dimensional network and some of the carboxylate groups form an ester bond, thus leading to the decrease of the band at 1515 cm⁻¹. Moreover, most of the newly formed ester bridges are expected to be more strained, and this could explain the increase of the peak at 1680–1750 cm⁻¹ and its shift to higher frequencies.

Finally, we considered the hypothetical (—O)₃Si—COOH species, modeling it with an isolated (OH)₃SiCOOH molecule, **7** (Figure 3). Among all the hypothesized solid-state species, the (—O)₃Si—COOH one is probably the less affected by solid structure effect so that its behavior is expected to be well reproduced by the corresponding molecular model. The geometrical optimization of **7** leads to the results reported in Tables 1 and 2. We see that the C=O stretching has been calculated

at 1691 cm⁻¹, in good agreement with the observed frequency at 1705 cm⁻¹.

4.3. Thermodynamic Considerations. We have also considered the energetics of the formation of the proposed species from the *E'* defects and CO₂ and the thermodynamic stability of these silicon carboxylate derivatives.

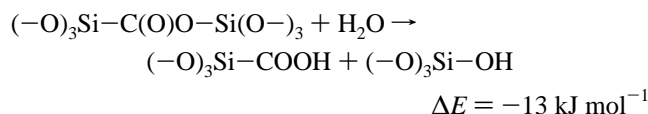
The main hypothesis of the above interpretation is the essentially simultaneous formation of (i) an ionic pair constituted by a carboxylate anion and a silicon cation and (ii) a silicon–silicon bridging ester species. The formation energy ΔE for these two reactions has been calculated as



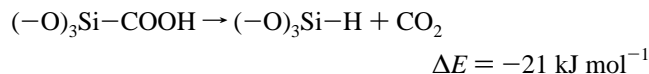
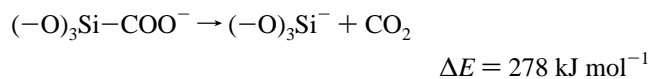
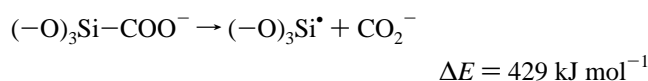
We see that the formation of the $(-\text{O})_3\text{SiCOO}^-$ and $(-\text{O})_3\text{Si}^+$ isolated ions from two $(\text{OH})_3\text{Si}^\bullet$ radicals and a CO₂ molecule is a strongly endothermic process (+478 kJ mol⁻¹). The formation of a carboxylate ion is therefore possible only because of an electrostatic energy stabilizing the ionic pair. A proper evaluation of the energy for such an ionic pair species would require a more accurate level of calculation and has not been faced. However, even from elementary electrostatic considerations it follows that, describing the ionic charges as pointlike, the ionic adduct is expected to be stable when the cation–anion distance is less than ca. 4.0 Å.

A strongly exothermic formation energy (412 kJ mol⁻¹) is calculated for the esterlike species, in agreement with the experimental evidence that silicon carboxylate anions form ester species after annealing. However, this value is significantly reduced by strain effects in lower cyclic silicon ester species, and this can explain why only a part of the silicon carboxylate species form ester bonds in the as-prepared sample without heat treatment. For instance, the formation energy of the three membered cyclic molecule **6** from CO₂ and the $(\text{OH})_2\text{Si}^\bullet\text{O}-\text{Si}(\text{OH})_2-\text{O}-\text{Si}(\text{OH})_2$ diradical is 378 kJ mol⁻¹, while that of the two-membered cyclic molecule **5** from CO₂ and the $(\text{OH})_2\text{Si}^\bullet\text{O}-\text{Si}(\text{OH})_2$ diradical is 336 kJ mol⁻¹.

Despite its high formation energy, the ester bond is thermodynamically unstable with respect to the reaction with water, leading to a silicon carboxylic acid and a silanol:



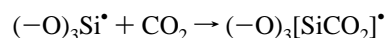
As no molecular silicon carboxylate derivatives have been synthesized to date, we have considered the theoretical stability of the silicon carboxylate **3** and carboxylic acid **7** model molecules. First of all, the stability of these molecules is supported by the following observations: (i) the geometry optimizations performed on both molecules lead to true minima of the potential energy surface, and (ii) the harmonic normal-mode analysis shows real frequencies for rather well localized Si–C stretching modes in the range 1000–1100 cm⁻¹. To give a more quantitative measure of the stability of these molecules, we considered the reaction leading to the chemically most reasonable fragments:



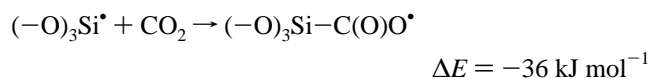
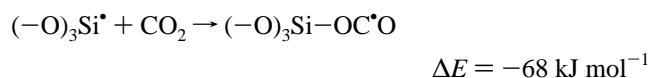
We see that the carboxylate ion is stable with respect to the above fragmentations, while the carboxylic acid is unstable, although by a very small energy amount. However, we should take into account that the latter fragmentation reaction involves the initial breaking of a Si–C bond and is therefore expected to require a high activation energy. The performed calculations therefore indicate the stability of these silicon carboxylate derivatives molecular models, thus confirming the stability of the solid-state species.

As cited above, the molecular organosilicon carboxylic derivatives are not known and are considered to be unstable. Indeed, although several thousands of organosilicon compounds are known,²⁴ only few compounds have been characterized in which the carbon atom bound to the silicon is part of a highly electron-attracting functional group (as in COOH, COOR, COO⁻, CONH₂, etc.). The effect of these substituents is to increase the already high polarity of the Si–C bond and make it extremely susceptible to an electrophilic attack.²⁵ Our calculations indicate that this instability is of a kinetic, rather than thermodynamic, origin and that the silicon–carbon bond is in principle still quite stable. The stabilization of these reactive species within the dispersed silica is due to the prevention of the attack of the Si–C bond by solvent or other molecular fragments which are unavoidable in gas phase or in solution. In a way, their stabilization in a SiO₂ skeleton is equivalent to the protection by infinitely bulky steric groups. Therefore, ion bombardment of highly dispersed solids provides a new tool for fundamental studies of stability and reactivity of molecules.

4.4. Isolated Silicon Radicals and Mechanism of the Ester Bridge Formation. Although the reactivity of ion-irradiated silica is due to an adjacent pair of $(-\text{O})_3\text{Si}^\bullet$ radicals, it is interesting to consider also an isolated silicon radical, modeled by a $(\text{OH})_3\text{Si}^\bullet$ molecular species. Such a radical center interacts with CO₂ to give a radical adduct.⁷



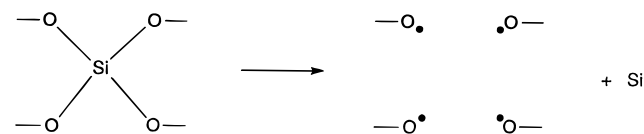
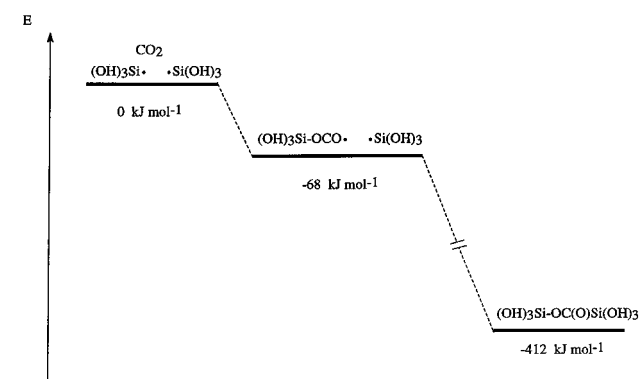
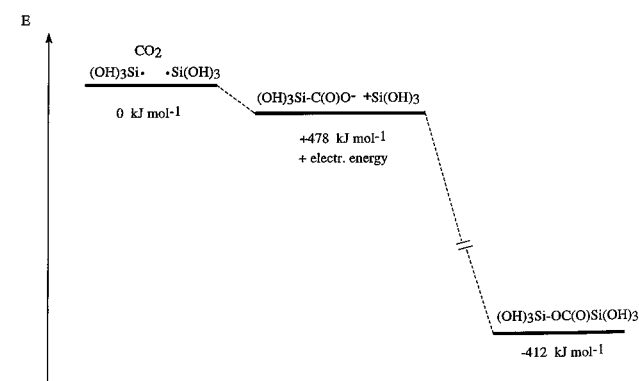
We modeled this radical center by a $(\text{OH})_3\text{Si}^\bullet$ molecular species and considered both the possible oxygen-attached $(\text{OH})_3\text{Si}-\text{OC}^\bullet\text{O}$, **8**, and carbon-attached $(\text{OH})_3\text{Si}-\text{C}(\text{O})\text{O}^\bullet$, **9**, radical adducts. A geometry optimization has been performed on **8** and **9** and the results are reported Table 5. The following formation energies are obtained for these species



and show that the oxygen-attached adduct is 32 kJ mol⁻¹ more stable than the carbon-attached one, at variance with the results observed for the analogue anion species **2** and **3** (see section 4.2), which give unstable oxygen-attached carboxylate adducts **2**. Notice that the results above are in good agreement with the experimental investigations of Radtsig and co-workers which attributed to the $(-\text{O})_3[\text{SiCO}_2]^\bullet$ radical adduct the oxygen-attached structure $(-\text{O})_3\text{Si}-\text{OC}^\bullet\text{O}$ rather than the carbon

TABLE 5: Main Optimized Geometrical Parameters for the Model Molecules 8 and 9

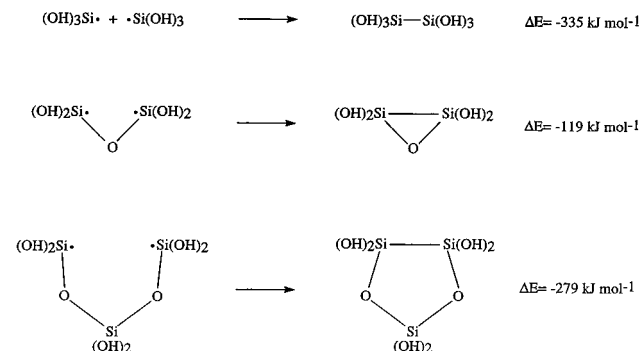
	8	9
Si—C		2.07
Si—O(CO)	1.76	
C—O	1.21/1.33	1.23
Si—O(H)	1.68	1.69
(Si)O—H	0.98	0.98
O—C—O	139	144
Si—O—C	114	
Si—C—O		115
O—Si—O	115	
C—Si—O		116
Si—O—H	101	102

SCHEME 2**SCHEME 3****SCHEME 4**

attached structure $(-\text{O})_3\text{Si}-\text{C}(\text{O})\text{O}^\bullet$, giving for it a formation energy of 75 kJ mol^{-1} from the silicon radical and the CO₂ molecule. The stability of the radical species **8** suggests a radical mechanism for the formation of an ester bridge between the silicon centers of E'' defects in the as-implanted sample, according to which one of the two silicon radicals of the defect forms the radical adduct $(-\text{O})_3\text{Si}-\text{OC}^\bullet\text{O}$, which then recombines, through the carbon atom, with the adjacent $(-\text{O})_3\text{Si}^\bullet$ radical (see Scheme 3).

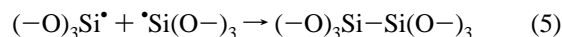
An ionic mechanism is also possible according to which the interaction of the CO₂ with the two vicinal silicon radicals of an E'' defect leads to a $(-\text{O})_3\text{Si}-\text{COO}^- + \text{Si}(\text{O}-)_3$ ionic pair, which then relaxes to the ester species (see Scheme 4).

Note that the ionic pair is stable only due to the electrostatic interaction, and its formation energy is expected to be negative for Si—Si distances shorter than ca. 4 \AA .

SCHEME 5

Since the ionic pair electrostatic interaction depends on the distance between the two silicon centers of the E'' defect, the latter geometric parameter can discriminate critically between the two possible mechanisms. In the limiting case in which the relaxation of the native defects leads to a silicon—silicon distance not compatible with the formation of the ester bridge, a stable ionic pair is formed and a carboxylate species is experimentally detected.

4.5. Recovery of the E'' Center. As the E'' center associated with the oxygen bridge vacancy is made up by two close silicon radicals, a simple recovery mechanism is available with the formation of a bond between the two silicon atoms,



However, the formation of a Si—Si bond can actually occur only if the energy gained in this process exceeds the energy required to strain the SiO₂ skeleton. In the above situation, the CO₂ insertion between the silicon atoms is obviously prevented. Although the presence of a Si—Si bond cannot be detected in an IR investigation (the Si—Si stretching frequency falls around 800 cm^{-1} , in a spectral region covered by the SiO₂ skeletal vibrations), it is interesting to study the energetics of the formation of a silicon silicon bond. Moreover, to evaluate the strain effect of the silica network on this bond formation energy, we considered the formation of a Si—Si bond between two free $(\text{OH})_3\text{Si}^\bullet$ radicals and between the two terminal silicon atoms of a $(-\text{O})_2\text{Si}^\bullet-\text{O}-\bullet\text{Si}(\text{O}-)_2$ and a $(-\text{O})_2\text{Si}^\bullet-\text{O}-\text{Si}(\text{OH})_2-\text{O}-\bullet\text{Si}(\text{O}-)_2$ diradical species (see Scheme 5). This allows us to simulate the recovery of the E'' center formed by oxygen displacement in two- and three-membered ring structures of the silica network. The results below show that the Si—Si bond energy is 335 kJ mol^{-1} when a complete relaxation of the two $\text{Si}(\text{OH})_3$ groups is allowed and, although substantially reduced by strain effects in cyclic species, remains fairly high in the three- and two-membered cycles (279 and 119 kJ mol^{-1} , respectively). This analysis shows that the energetic convenience of the E'' center recovery in a cycle with n silicon atoms increases with n (the acyclic system in which the two $\text{Si}(\text{OH})_3$ groups are left free can be considered as the limiting case of a cycle with $n \rightarrow \infty$). An analogous situation was found in the previous section for the formation of a $-\text{C}(\text{O})\text{O}-$ bridge in cyclic species. The results show that, for cycles with the same number n of silicon atoms, the formation of a $-\text{C}(\text{O})\text{O}-$ bridge is energetically favored over the formation of a Si—Si bond by almost 100 kJ mol^{-1} . This shows the thermodynamic preference of the E'' center to ester bond formation than to recovery, in agreement with the experimental evidence for such species.

5. Conclusions

In this work quantum chemical modeling is applied to interpret the results of an experimental infrared characterization

of the addition of CO₂ to the SiO₂ skeleton at the diradical silicon defect produced by argon bombardment. Accurate DFT calculations have been performed on suitable models of the silica E'' defect and their CO₂ adducts. The results are consistent with a previous interpretation of the IR data, according to which the addition of CO₂ takes place first via the formation of a carboxylate group which, after annealing, evolves to an ester species and then to a carboxylic acid after exposure to wet air. The calculations show that the proposed silcon carboxylate derivatives are stable species and yield C—O stretching frequencies in quantitative agreement with the experimentally observed values.

Ion bombardment of highly dispersed solids provides a new tool for fundamental studies of stability and reactivity of molecules. The advantage of the technique is that the site can be very reactive and even highly energetic, the drawbacks being the difficulties of characterization of these species. In this context the use of accurate theoretical methods is very useful to study the geometric structure and the thermodynamic stabilities of these species otherwise unavailable by experimental studies.

Acknowledgment. We thank Dr. L. Meda (Istituto Donegani) for helpful comments.

References and Notes

- (1) Brinker, C. J.; Scherer, G. W., *Sol-Gel Science*; Academic Press: London 1990.
- (2) Morterra, C.; Low, M. J. D. *J. Phys. Chem.* **1969**, *73*, 327.
- (3) Borello, E.; Zecchina, A.; Morterra, C.; Low, M. J. D. *J. Phys. Chem.* **1967**, *71*, 2938.
- (4) Low, M. J. D.; Rhodes, Y. E.; Orphanos, P. D. *J. Catal.* **1975**, *40*, 236.
- (5) Pauthe, M.; Phalippou, J.; Corriu, R.; Leclercque, D.; Mutin, P. H.; Vioux, A. *J. Non-Cryst. Solids* **1990**, *113*, 21.
- (6) Belot, V.; Corriu, R.; Leclercque, D.; Mutin, P. H.; Vioux, A. *Chem. Mater.* **1991**, *3*, 127.
- (7) Radsig, V. A.; Bystikov, A. V. *Kinet. Katal.* **1978**, *19*, 713. Radsig, V. A. *Kinet. Katal.* **1979**, *20*, 448. Radsig, V. A. *Kinet. Katal.* **1979**, *20*, 456. Radsig, V. A.; Khalif, V. A. *Kinet. Katal.* **1979**, *20*, 705.
- (8) Cerofolini, G. F.; Meda, L.; Spaggiari, C.; Conti, G.; Garbasso, G. *M. J. Chem. Soc., Faraday Trans.* **1996**, *92*, 2453.
- (9) Cerofolini, G. F.; Anselmino, A.; Meda, L.; Ranghino, G. *Mater. Res. Soc. Symp. Proc.* **1996**, *431*, 303.
- (10) Sauer, J. *Chem. Rev.* **1989**, *89*, 199.
- (11) Sulimov, V. B.; Pisani, C.; Corá, F.; Sokolov, V. O. *Solid State Commun.* **1994**, *90*, 511.
- (12) Sauer, J.; Ugliengo, P.; Garrone, E.; Saunders, V. R. *Chem. Rev.* **1989**, *89*, 199.
- (13) Garrone, E.; Ugliengo, P. In: *Structure and Reactivity of Surfaces*; Zecchina, A.; Costa, G.; Morterra, C., Eds.; Elsevier: Amsterdam, 1989.
- (14) Ugliengo, P.; Saunders, V. R.; Garrone, E. *J. Phys. Chem.* **1989**, *93*, 5210.
- (15) Frisch, M. J.; Trucks, G. W.; Schlegel, H. M.; Gill, P. M. W.; Johnson, B. G.; Wong, M. W.; Foresman, J. B.; Robb, M. A.; Head-Gordon, M.; Replogle, E. S.; Gomperts, R.; Andres, J. L.; Raghavachari, K.; Binkley, J. S.; Gonzales, C.; Martin, R. L.; Fox, D. J.; Defrees, D. J.; Baker, J.; Stewart, J. J. P.; Pople, J. A. *Gaussian 94*, Revision A.1; Gaussian Inc.: Pittsburgh, PA, 1994.
- (16) Vosko, S. H.; Wilk, L.; Nuisar, M. *Can. J. Phys.* **1980**, *58*, 1200.
- (17) Becke, A. D. *Phys. Rev.* **1988**, *A38*, 2398.
- (18) Lee, C.; Young, W.; Parr, R. G. *Phys. Rev.* **1988**, *B37*, 785.
- (19) Ziegler, T. *Chem. Rev.* **1991**, *91*, 651.
- (20) Ziegler, T. *Can. J. Chem.* **1995**, *73*, 743.
- (21) Wong, M. W. *Chem. Phys. Lett.* **1996**, *256*, 391.
- (22) Sheldon, J. C.; Bowie, J. H.; DePuy, C. H.; Damrauer, R. *J. Am. Chem. Soc.* **1986**, *108*, 6794.
- (23) Bellamy, L. J. *The Infrared Spectra of Infrared Molecules*; Chapman and Hall: London, 1975; Vol. 1.
- (24) Bazant, V.; Chvalovsky, V.; Rathousky, J. *Organosilicon Compounds*; Czech. Acad. Sci.: Prague; and Academic Press: New York, 1965.
- (25) Ebsworth, E. A. V. *Volatile Silicon Compounds*; Pergamon Press: London, and Macmillan Co.: New York, 1963.